Evaluation of streak metal artifacts in cone beam computed tomography by using the Gumbel distribution: a phantom study

Yoshikazu Nomura, DDS, PhD,[a] Hiroshi Watanabe, DDS, PhD,[a] Nisha Gowri Manila, BDS, PhD,[b] Sakurako Asai, DDS, PhD,[a] and Tohru Kurabayashi, DDS, PhD[a]

Objective. The aim of this study was to confirm whether streak metal artifacts (SMAs) between titanium implants on cone beam computed tomography (CBCT) images could be evaluated by using the Gumbel distribution (GD). Moreover, the influence of different scan settings on SMAs was investigated.

Study Design. An iodine solution simulating dentin was placed between 2 titanium rods in an acrylic phantom. It was scanned by using CBCT at 2 settings with nearly equivalent exposure doses (90 kV, 7 mA; 78 kV, 10 mA). The images were analyzed, and the dependence of the voxel values in SMAs on GD was investigated with the coefficient of determination (r^2). The location parameters, indicating the strength of the SMAs, were calculated for each scan setting and evaluated with the Mann-Whitney U test. Significance was established at $p = .05$.

Results. The SMAs on CBCT images depended on GD ($r^2 \geq .959$). The SMAs with the 78 kV, 10 mA settings were significantly smaller than those with the 90 kV, 7 mA settings ($p < .01$).

Conclusions. SMAs on CBCT images could be evaluated by using methods based on GD. The strengths of metal artifacts varied with changes in scan settings, even at nearly equivalent exposure doses. (Oral Surg Oral Med Oral Pathol Oral Radiol 2021;131:494−502)

Cone beam computed tomography (CBCT) as used in dentistry provides higher spatial resolution, lower x-ray dose, and reduced cost compared with multidetector computed tomography (MDCT). CBCT is an essential tool that is often used for assessment and treatment planning for dental implants, endodontic therapy, and oral surgery.[1-4] Therefore, various studies have been conducted on the image quality of CBCT scans.

One severe limitation of CBCT is the presence of metal artifacts. Image noise appears when a metal exists between the x-ray tube and the detector during scanning.[5] This phenomenon results from the fact that the x-ray absorption coefficient of metals is very high and leads to image reconstruction problems.[6] It is difficult to avoid the interference from metal artifacts in CBCT images after titanium implant placement. In particular, streak metal artifacts (SMAs) appear in the area between 2 implants and often adversely affect diagnostic accuracy. The SMAs between titanium implants sometimes make it difficult to evaluate root fractures, root resorption, or bone resorption.

The scan parameters of tube voltage and tube current are adjustable in many CBCT devices.[5,7] However, evidence for the optimal scan setting to reduce SMAs quantitatively is currently insufficient. Imai et al. described a method to evaluate streak artifacts on MDCT images.[8] The profiles—the value change of voxels between 2 positions—perpendicular to the streak artifacts were investigated and analyzed with a focus on the largest difference between the CT numbers of adjacent pixels in each profile. The largest differences in the profiles were dependent on the Gumbel distribution (GD), which is one of the 3 types of generalized extreme value distributions.[8-10] (Type I is GD, type II is the Fréchet distribution, and type III is the Weibull distribution.) An extreme value distribution is one of the continuous probability distributions, sometimes observed as the distribution of the maximum or minimum values of groups in particular circumstances. In GD, a mode is indicated as a location parameter; the values of the 2 groups dependent on GD can be compared by using the location parameters. Imai et al. stated that location parameters indicate the strengths of the noise quantitatively.[8] The characteristics of their method were suitable to evaluate streak artifacts—quantitative, easy to use in the comparison of various conditions, and insusceptible to other artifacts.[8,10-12] These authors also prepared an evaluation procedure to confirm whether the obtained data of the streak artifacts could be evaluated by the method based on GD.[8,10-12] Additional findings regarding MDCT scans have been identified in the studies derived from their method.[8,10-15]

Statement of Clinical Relevance

Optimized tube voltage and tube current may reduce metal artifacts between titanium implants in cone beam computed tomography without changing the exposure dose. The metal artifacts can be evaluated quantitatively by using the Gumbel distribution.

[a]Oral and Maxillofacial Radiology, Graduate School, Tokyo Medical and Dental University, Tokyo, Japan.
[b]Oral and Maxillofacial Radiology, Department of Diagnostic Sciences, Texas A&M College of Dentistry, Dallas, TX, USA.
Received for publication Mar 31, 2020; returned for revision Jul 11, 2020; accepted for publication Aug 15, 2020.

2212-4403/$-see front matter
https://doi.org/10.1016/j.oooo.2020.08.031

To our knowledge, no study has analyzed CBCT images with the use of GD. Moreover, it is unknown whether the SMAs on the tooth root between 2 implants could be evaluated quantitatively on the basis of GD. Hence, this study had 2 aims: to confirm whether SMAs in CBCT images simulating the scan of dentin located between 2 implants can be evaluated on the basis of GD, and to investigate the influence of changing tube voltage and current on the strength of SMAs.

MATERIALS AND METHODS

Scan target

A phantom consisting of acrylic resin and water was employed to simulate the human head in the present study.[4,7,16] We used an iodine solution to simulate the CT or Hounsfield number (HU) of dentin. This is a completely homogeneous material and allowed us to reproduce the radiodensity of dentin. The heterogeneity of a scan target can interfere with the evaluation of the variations in voxel value caused by image noise.[4] Iodine solution was also easy to obtain because it is used as a contrast agent in radiology.[7,16] Based on findings from previous research and our preliminary experiments, the solution concentration was set at 75 mgI/mL.[17,18] The solution was placed into a polyethylene box (height 42 mm × width 16 mm × depth 16 mm) and positioned between 2 titanium rods (diameter 4 mm × length 40 mm). The rods were located on the left periphery in the water container (diameter 80 mm × height 81 mm). Two acrylic columns (diameter 80 mm × height 60 mm) were placed on and under the water container; these were inserted into the circular opening (diameter 82 mm × depth 185 mm) of the acrylic phantom (diameter 160 mm × height 200 mm). The central axis of the opening was positioned ahead (29 mm) of that of the acrylic phantom. A diagram and photograph of the phantom are shown in Figure 1.

MDCT scan to measure the HU of the iodine solution

To validate that the CT number of the 75 mgI/mL iodine solution was close to that of dentin, MDCT was performed with a Somatom Sensation 64 unit (Siemens Healthineers, Erlangen, Germany). The iodine solution placed in the acrylic phantom was scanned once without the titanium rods. The MDCT settings were 120 kV, 140 effective mAs, a pitch of 0.6, and a rotation speed of 1 rotation/second, identical to the parameters used for our clinical cases. The acrylic phantom was laid on the bed of the MDCT scanner. Its front was oriented above the bed. The central axis of the acrylic phantom was set to the rotation center of the gantry. The image data were reconstructed as axial sections with a thickness of 0.6 mm by using the reconstruction kernel H40s. The axial image at the middle level of the iodine solution box was exported in the DICOM (Digital Imaging and Communications in Medicine) format. The data were imported to a WEASIS Media Viewer 3.0.1 (Weasis Team), an open-source DICOM viewer. The region of interest (ROI) with a round shape (diameter 11 mm) was set on the iodine solution in the axial image, and the average CT number was measured. The iodine solution had a CT number of 1742 HU. Yampri et al. reported that the CT number of dentin was 1100 to 2000 HU.[17] Matsuyama et al. reported that it was approximately 1,800 HU.[18] Hence, the iodine solution scanned in this study could be considered a valid material to simulate dentin.

CBCT scan

A 3D Accuitomo FPD 8 (J. Morita Mfg. Corp., Kyoto, Japan) was employed as the CBCT apparatus. The scan settings were selected for a rotation of 360 degrees (scan time: 17.5 seconds) and a field of view of 4 × 4 cm for each CBCT scan. The following 2 settings with similar radiation doses were selected for tube voltage and tube current:

Setting (I): 90 kV, 7 mA, with a volume computed tomography dose index of 3.59 mGy.

Setting (II): 78 kV, 10 mA, with a volume computed tomography dose index of 3.58 mGy.

The acrylic phantom was scanned once with each scan setting. The center of the iodine solution was positioned at the isocenter of the field of view in each scan. The image data were reconstructed as axial images with a slice thickness of 0.32 mm and a slice interval of 0.16 mm and exported in DICOM format. The 10 axial images around the middle level of the iodine solution acquired with settings (I) and (II) were evaluated.

Analysis based on GD

The image data were analyzed by using GD on the basis of the method described by Imai et al.[8,12] The procedure was as follows:

Setting of the profiles perpendicular to the artifacts. The DICOM data were imported into the original software developed by us with Delphi (Embarcadero, TX) and Visual Studio (Microsoft, Redmond, WA). Through the use of the software, 170 profiles with a length of 56 voxels were set on the iodine solution perpendicular to the line connecting the 2 titanium rods in each axial image. The contrast values of the iodine solution and the water outside the SMAs were measured as a reference. Rectangular ROIs (width 40 voxels × height 120 voxels) were set on the iodine solution (outside the region between the 2 titanium rods) and on the adjacent water to calculate the contrast values. These profiles and ROIs were set by a radiologist (dentist) with a doctoral degree in dentistry

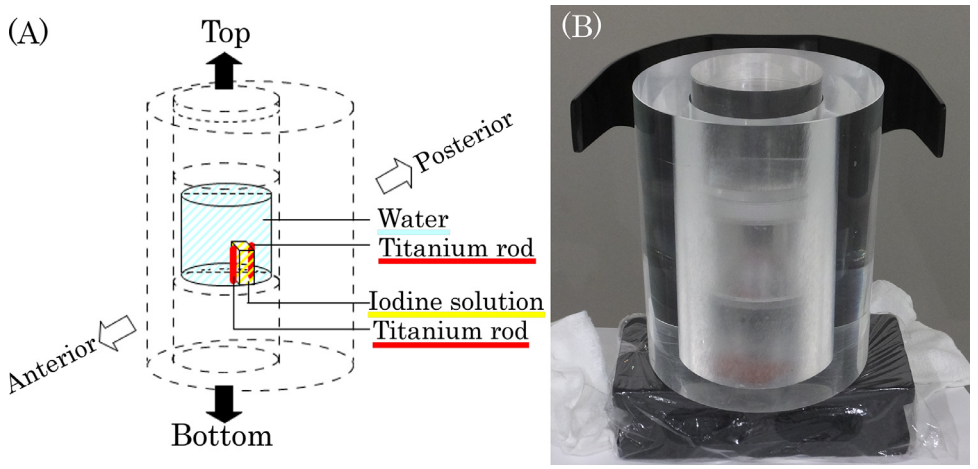

Fig. 1. The acrylic phantom used in this study (diameter 160 mm × height 200 mm). **(A)** Diagram of the phantom. **(B)** Photograph of the phantom placed in front of the headrest of the cone beam computed tomography apparatus. A water container was inserted (diameter 80 mm × height 81 mm) in a circular opening. An iodine solution box (height 42 mm × width 16 mm × depth 16 mm) was placed between 2 titanium rods (diameter 4 mm × length 40 mm) at the left peripheral location in the water container to simulate the molar region.

and approximately 10 years of experience in CBCT radiology. The averaged voxel values were obtained in the respective ROIs. The difference between the averaged voxel values of the iodine solution and water was calculated and regarded as the contrast of the image. Each position of the ROIs is shown in Figure 2.

Sampling of the largest difference between adjacent voxel values in each profile. Because a profile consisted of 56 voxels in this study, the absolute values of the 55 differences between adjacent voxel values were calculated, with the largest value extracted in each profile. The largest value was divided by the contrast value calculated from the iodine solution and water in each image and recorded in each profile. The recorded values in each image were sorted in ascending order. Hereafter, the group of values in the image is termed $x_1, x_2, \ldots x_{170}$.

Evaluation based on GD. To investigate whether the values of $x_1, x_2, \ldots x_{170}$ depended on GD, their conformity with the following numerical expression (1) of GD was evaluated:

$$F(x) = exp(-exp(-(x-\beta)/\gamma)) \quad (1)$$

$F(x)$: Cumulative probability when the largest difference in each profile is x

β: Location parameter

γ: Scale parameter

A location parameter and a scale parameter indicate the mode and variance of x in GD, respectively. Hence, a location parameter can be treated as an index of the strength of the artifact. Formula (1) is convertible by applying the double logarithm to both the left and right sides of the equation:

$$-ln(-ln\ F(x)) = x/\gamma - \beta/\gamma \quad (2)$$

If $x_1, x_2, \ldots x_{170}$ were linearly related to $-ln(-lnF(x_1)), -ln(-lnF(x_2)), \ldots -ln(-lnF(x_{170}))$, $x_1, x_2, \ldots x_{170}$ could be considered to depend on GD according to formula (2). The ideal values of $F(x)$ can be calculated by using the mean rank method, and $F(x)$ is convertible as follows:

$$F(i) = i/(n+1)$$

i: Order of largest difference (1, 2, ... 170 in the present study)

n: Number of samples (170 in the present study)

Hence, the dependency on GD could be evaluated by plotting $[x_1, -ln(-ln(1/171))]$, $[x_2, -ln(-ln(2/171))]$, ... $[x_{170}, -ln(-ln(170/171))]$ and calculating a correlation coefficient. This plotting is called the *Gumbel plot*. If the plot shows linearity, $x_1, x_2, \ldots x_{170}$ can be approximated by GD. When the regression line of the scatter plot is $y = ax + b$, the location parameter β of GD is calculated as follows according to formula (2):

$$\text{location parameter } \beta = -b/a$$

The location parameter can be considered to indicate the strength of the artifact. As above, the correlation coefficients (r) and the location parameters were calculated in each slice produced with scan settings (I) and (II).

Statistical analysis of the location parameters. The r^2 (the square of the correlation coefficient or the coefficient of determination) was calculated to measure how

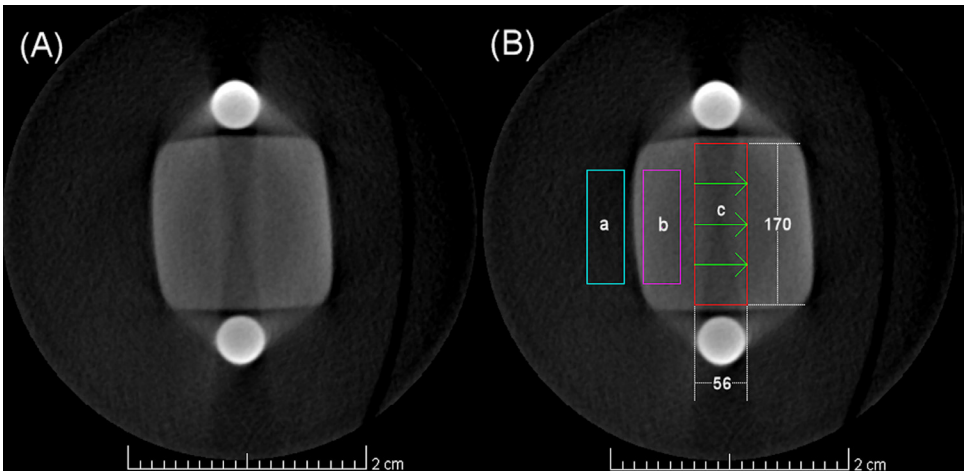

Fig. 2. Region of interest (ROI) settings to calculate contrast values and profiles on a streak metal artifact. **(A)** An original image. **(B)** a. ROI for water. b. ROI for iodine solution. c. Position of 170 profiles (length 56 voxels) set on a streak metal artifact. The directions of all profiles were perpendicular to the line connecting the 2 titanium rods. The difference between the averaged voxel values in water and iodine solution was used to calculate the contrast in each image. The ratio of the largest difference of adjacent voxel values in each profile to the contrast was used for the calculation of a location parameter.

well GD predicts the largest differences between voxels. The Mann-Whitney U test was applied to the location parameters (n = 10 in each setting) to evaluate the difference in artifacts between the 2 scan settings.[19] GNU R (R Development Core Team) was used for statistical analysis. Significant difference was established at p = .05.

RESULTS

Profiles perpendicular to the SMAs

In this study, 3400 profiles (170 profiles × 10 images × 2 settings) were investigated, as shown in Figure 3. The largest difference between the adjacent voxel values was calculated in each profile; that is, all the differences between the adjacent voxel values were confirmed to be not greater than the largest difference.

Contrast between the iodine solution and water

The largest differences between the adjacent voxel values were recorded as the ratios to the contrast between the iodine solution and water. The mean and standard deviation (SD) of 10 contrast values measured from 10 images of scan setting (I) were 625.2 and 1.3,

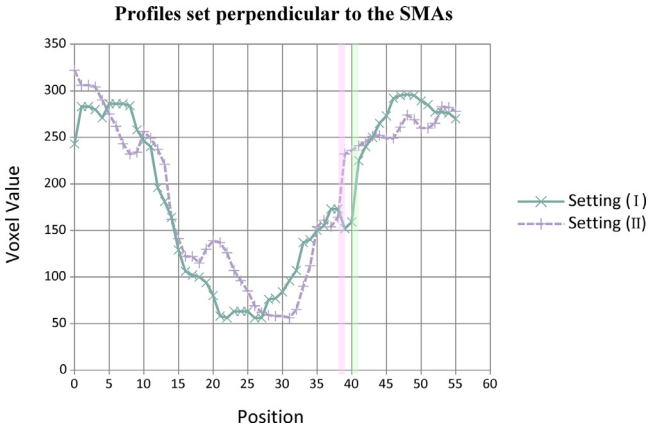

Fig. 3. Examples of the profiles in this study. The x-axis indicates the voxel position (0: Right; 55: Left). The graph shows the profiles running near the center of the middle level of the iodine solution in scan settings (I) and (II). Setting (I): 90 kV, 7 mA. Setting (II): 78 kV, 10 mA. The largest difference between adjacent voxel values was calculated in each profile; that is, all the differences between the adjacent voxel values were confirmed to be not greater than the largest difference. In the graph, the positions of the largest differences produced with scan settings (I) and (II) were 40−41 and 38−39, respectively, as indicated by the green and violet vertical lines.

Table I. Voxel values of iodine solution and water, with calculated contrast values

Scan setting	*(I)*			*(II)*		
	Iodine solution	*Water*	*Contrast*	*Iodine solution*	*Water*	*Contrast*
Mean	**362.0**	**−263.2**	**625.2**	**384.8**	**−229.2**	**614.0**
Median	361.9	−263.2	624.9	384.6	−229.2	613.8
Standard deviation	**0.6**	**0.9**	**1.3**	**1.0**	**0.5**	**1.5**
Maximum	363.1	−261.8	627.5	386.7	−228.4	616.5
Minimum	361.2	−264.9	623.8	383.5	−230.2	612.2

Note: Average voxel values of a 75 mgI/mL iodine solution and water in each axial image with the settings (I): 90 kV, 7 mA and (II): 78 kV, 10 mA. (Note that the "Mean" is the mean of the 10 averaged voxel values.) Contrast was calculated as the difference between the average voxel values of the iodine solution and water in each axial image. The CT number (1742 Hounsfield unit) of the iodine solution was close to that of dentin as reported previously.

respectively. Those of the images made with scan setting (II) were 614.0 and 1.5, respectively (Table I).

Plotting based on GD

Plotting based on GD was performed for the 10 images in each scan setting. The r^2 ranged from 0.979 to 0.997 (median = 0.990) in scan setting (I) and from 0.959 to 0.994 (median = 0.989) in scan setting (II). The high r^2 values indicated a very dependable relationship between the largest differences in the profiles and GD.[20] Scatter plots of the axial slice at the middle level with each scan setting are shown in Figure 4.

Location parameters as the strength of artifacts

The location parameters ranged from 0.089 to 0.096 (median = 0.092) in setting (I) and from 0.083 to 0.095 (median = 0.087) in setting (II). The box plots of the data are shown in Figure 5. Results of the Mann-Whitney U test indicated that the location parameters from setting (I) were significantly higher than those from setting (II) ($p = .003$).

DISCUSSION

Metal artifacts are a severe limitation of CBCT. As shown in Figure 6, which contains CBCT images from our preliminary experiment, the SMA appears between 2 metal materials. This noise is often intense and can impede accurate diagnosis.

In the present study, the homogeneous iodine solution between the 2 titanium rods was scanned with settings (I) and (II) by CBCT to evaluate SMAs. With the original software developed for this study, 170 profiles perpendicular to the SMAs between the titanium rods were analyzed in each image. The largest differences between adjacent voxel values in each profile were measured, and their dependency on GD was evaluated.

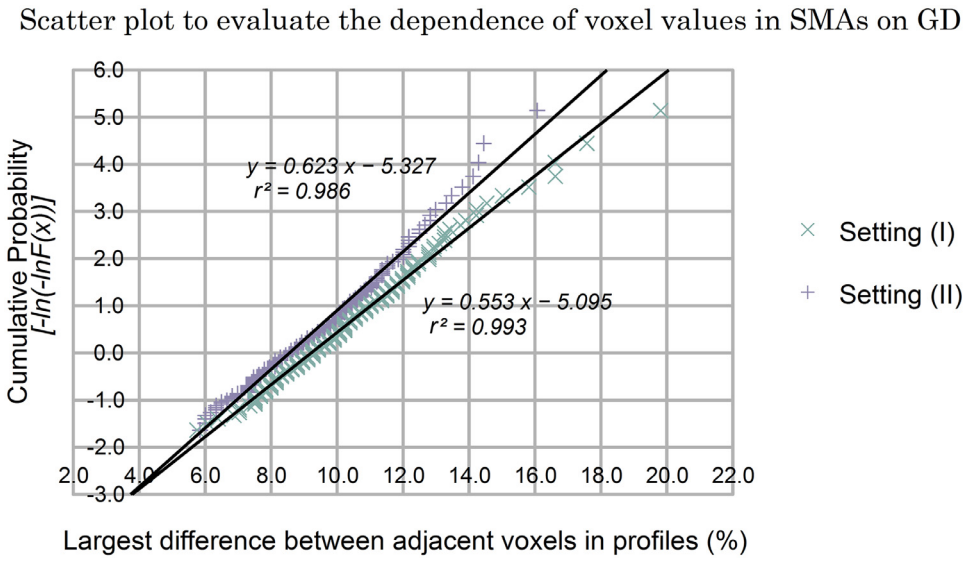

Fig. 4. The scatter plots to confirm whether the largest differences in the profiles on the image depended on the Gumbel distribution. The graph shows the data of the axial images at the middle level with scan settings (I) and (II). Setting (I): 90 kV, 7 mA. Setting (II): 78 kV, 10 mA. The linear relationship (indicated by the high coefficient of determination) indicated that a quantitative evaluation of the streak metal artifact by using location parameters was possible.

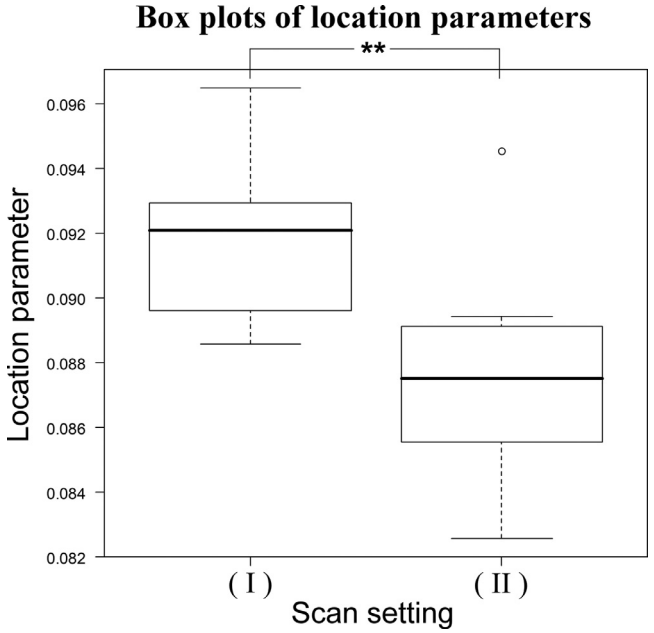

Fig. 5. Box plots of the location parameters in each image of the settings (I) and (II). ** $p < .01$. Setting (I): 90 kV, 7 mA. Setting (II): 78 kV, 10 mA.

Moreover, the influence of tube voltage and tube current on the SMAs between the rods was investigated by the location parameters as the strength of the SMAs.

The method employed in this study was based on that described by Imai et al., who found that the streak artifacts on MDCT images could be evaluated quantitatively by using GD.[8,12] Furthermore, various findings were revealed in subsequent investigations.[10-15] The characteristics of the method were suitable to evaluate streak artifacts and were quantitative, easy to use for comparison of various conditions, and insusceptible to other artifacts.[8,10-12]

The method of Imai et al. took account of reducing the influence of image noise unrelated to streak artifacts. The method was found to be reasonable for evaluation of streak artifacts for 2 reasons. First, the influence of noise in different directions from streak artifacts was reduced because the profiles were set perpendicular to the streak artifacts. Second, the influence of other noise in the same direction as the streak artifacts was also reduced relatively because only the largest differences of the adjacent voxels (at which the influence of the streak artifacts seemed to be the strongest) in the profiles were used to calculate the location parameters. We consider that Imai et al. took advantage of both the properties of the profile analysis and GD, which is sometimes observed in the group of maximum values.[10] Hence, we believe that the method of Imai et al. is reasonable for evaluating streak artifacts.

The method we employed in this study was almost the same as that of Imai et al.; however, we made a modification. They extracted the values of the largest differences of CT numbers between adjacent voxels in each profile, whereas we calculated the ratios of the largest differences to the contrast between the iodine solution and water. This was because the voxel values in CBCT are generally less quantitative than the CT numbers in MDCT.[4] In fact, they varied depending on changes in tube voltage, as shown in Table I. Therefore, we had to adopt the standardized values for the largest differences by calculating their ratios to the contrast between the iodine solution and water. The ROIs of the iodine solution and water were set near the SMA because voxel values of CBCT depend on the position in the axial image.[16] Because our method can be applied to both MDCT and CBCT, it can be considered to be more generalized than that of Imai et al.

We needed to confirm that the largest differences measured from each profile in this study depended on GD so that we could evaluate the strength of the artifacts by using location parameters. Thus, the r^2 was calculated between the largest differences and double logarithms of the ideal cumulative probabilities in each image (see Figure 4). The coefficient was very high in each image of both setting (I) and setting (II), and the largest differences depended on GD.[8,20] As a result, the location parameters were considered to indicate the strength of the artifacts in the present study.

The location parameters of scan setting (I) were significantly higher than those of scan setting (II) (see Figure 5). The results indicate that the artifacts in dentin-equivalent material placed between 2 titanium implants can be reduced by adopting a lower tube voltage and a higher

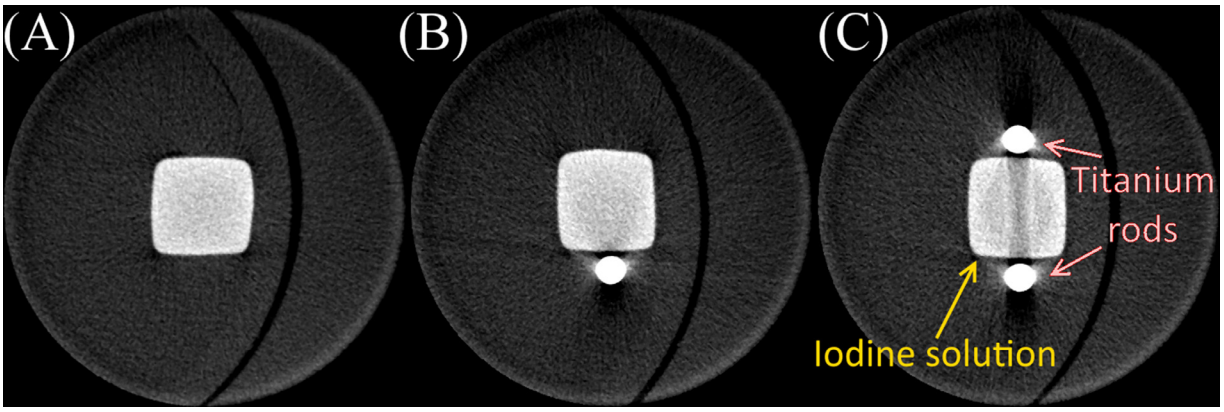

Fig. 6. The cone beam computed tomography image of a 75 mgI/mL iodine solution placed in an acrylic phantom with/without titanium rods, scanned in our preliminary experiment. **(A)** Without a titanium rod. **(B)** With 1 titanium rod. **(C)** With 2 titanium rods. The streak metal artifact appears between the 2 titanium rods.

tube current within a certain range when the radiation doses are equivalent. We considered 2 explanations for this phenomenon. The first was the characteristic change in the photons of x-rays. Lower tube voltage and higher tube current settings yield increasing numbers of photons with reduced energy per photon. The optimization of the balance between the number and energy of photons might improve the image reconstruction problems that occur when x-rays penetrate the titanium rods with their high absorption coefficient. The second explanation was the change in the scattered x-rays. Scattered radiation is one cause of the degradation of image quality[16] and decreases with lower tube voltage.[21] Its influence on the measurement of the largest differences in this study may be non-negligible.

The axial images at the middle level with settings (I) and (II) are shown in Figure 7. Their window width (the contrast of the images) and window level (brightness) were adjusted to directly compare the artifacts of 2 images. The authors judged that the artifact produced with setting (I) was somewhat stronger than that of setting (II) visually. However, it should be noted that the evaluation of image quality on paper depends on the quality of the paper and the printer, the observer, and the lighting. Similarly, the evaluation of image quality on a computer monitor depends on the quality and the settings of the monitor, the observer, and the lighting. Unlike subjective evaluations, the procedure using the location parameters in this study was a quantitative and objective evaluation.

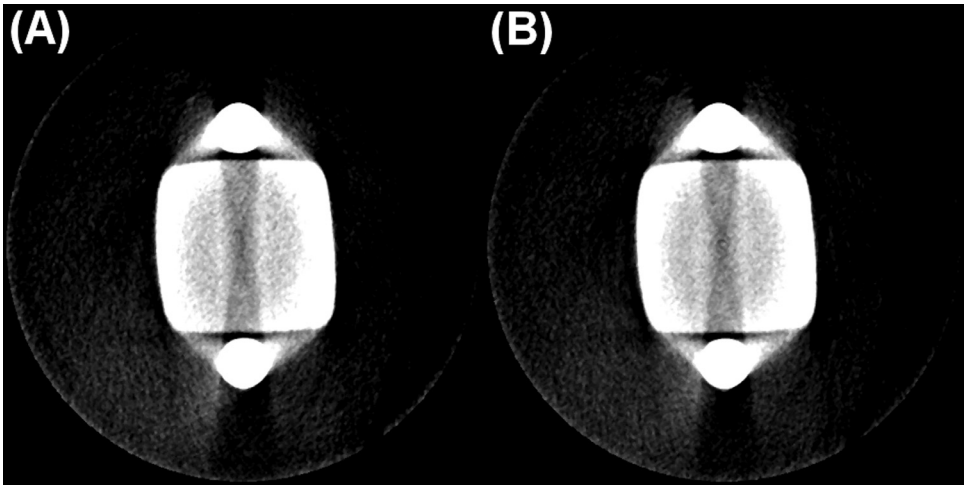

Fig. 7. Examples of images with streak metal artifacts (SMAs). **(A)** Axial image at the middle level (location parameter = 0.093) of the iodine solution scanned with setting (I): 90 kV, 7 mA. **(B)** Axial image at the middle level (location parameter = 0.086) of the iodine solution scanned with setting (II): 78 kV, 10 mA. The window level of each image was set to the mean of the average voxel values of the iodine solution and water. The window width was set to the difference between the average voxel values of the iodine solution and water. Hence, the strengths of SMAs between 2 titanium rods can be compared visually by using the gray depths in the 2 images; the authors considered that the SMA in **(A)** was somewhat stronger than that in **(B)**.

Metal artifacts are a significant issue in CBCT, and various studies have broached this topic. Katsumata et al. scanned blocks (10 × 10 × 20 mm) of various materials (e.g., aluminum/copper) inside a water phantom by using CBCT and evaluated the artifacts occurring inside the block.[22] They discovered that the artifacts were stronger with higher tube voltage. This observation was compatible with ours. Schulze et al. explained that metal artifacts result from inconsistencies in the processing of CT image reconstruction.[6] They scanned a phantom of plaster simulating a bone placed between 2 titanium rods located in a water tank (diameter 95 mm) using CBCT with 2 settings (80 kV, 4 mA; 90 kV, 4 mA). The decrease in voxel values on the plaster scanned with 80 kV, 4 mA was smaller than that scanned with 90 kV, 4 mA. Pauwels et al. scanned titanium and lead objects inside an acrylic phantom by using 13 CBCT devices and measured the SDs of the voxel values around the metal.[5] They discovered that with some CBCT systems, the SDs decreased significantly when the radiation dose was increased. This result suggests that the implementation of metal artifact reduction differs among CBCT manufacturers. Unlike these studies, our current research investigated whether the differences between 2 scan settings with nearly identical exposure doses affect the strength of metal artifacts. Bayrak et al. evaluated the effect of a metal artifact reduction algorithm and an adaptive image noise optimizer in the detection of peri-implant dehiscences with CBCT.[23] The GD-based method in the present study may be valuable when applied to the evaluation of such algorithms.

When designing in vitro experiments, researchers should be aware of the properties of materials that might be employed. In this study, we scanned an iodine solution, which is homogeneous, easy to obtain, and simulates the high density of hard tissue.[16] In our previous study, a urethane phantom mixed with hydroxyapatite was ordered as a scan target simulating cancellous bone (with a density lower than that of dentin); however, the phantom contained air bubbles.[4] Iodine solutions have been shown in other studies to be a useful material for making uniform and dense scan targets with CT numbers equivalent to dentin.[7,16,24,25]

The limitation of this study was that the evaluations were made with images acquired with only 1 CBCT apparatus. We strongly believe that further research is needed to test the generalizability of our findings.

CONCLUSIONS

The GD-based method of Imai et al. was suitable for evaluating streak artifacts in MDCT scans, and this study revealed that it could be applied to the evaluation of SMAs produced on CBCT scans. At nearly equivalent exposure doses, the scan settings of 78 kV and 10 mA caused weaker SMAs than those of 90 kV and 7 mA. These results might also apply to clinical cases. The GD-based method may be useful for optimizing scan settings to reduce metal artifacts in CBCT images.

FUNDING

This work was supported by JSPS KAKENHI Grant Numbers JS15K20382.

REFERENCES

1. Watanabe H, Wagatsuma T, Nomura Y, Honda E, Kurabayashi T. Spatial resolution of FineCube, a newly developed cone-beam computed tomography system. *Oral Radiol*. 2010;26:56-60.
2. Roberts JA, Drage NA, Davies J, Thomas DW. Effective dose from cone beam CT examinations in dentistry. *Br J Radiol*. 2009;82:35-40.
3. Sukovic P. Cone beam computed tomography in craniofacial imaging. *Orthod Craniofacial Res*. 2003;6:31-36.
4. Nomura Y, Watanabe H, Shirotsu K, Honda E, Sumi Y, Kurabayashi T. Stability of voxel values from cone-beam computed tomography for dental use in evaluating bone mineral content. *Clin Oral Implants Res*. 2013;24:543-548.
5. Pauwels R, Stamatakis H, Bosmans H, et al. Quantification of metal artifacts on cone beam computed tomography images. *Clin Oral Implants Res*. 2013;24:94-99.
6. Schulze RKW, Berndt D, D'Hoedt B. On cone-beam computed tomography artifacts induced by titanium implants. *Clin Oral Implants Res*. 2010;21:100-107.
7. Nomura Y, Watanabe H, Honda E, Kurabayashi T. Reliability of voxel values from cone−beam computed tomography for dental use in evaluating bone mineral density. *Clin Oral Implants Res*. 2010;21:558-562.
8. Imai K, Ikeda M, Wada S, Enchi Y, Niimi T. Analysis of streak artefacts on CT images using statistics of extremes. *Br J Radiol*. 2007;80:911-918.
9. Gumbel EJ. Statistics of extremes. Columbia University Press; 1958. Available at: https://catalog.hathitrust.org/Record/000226751. Accessed September 27, 2020.
10. Imai K, Ikeda M, Enchi Y, Niimi T. Statistical characteristics of streak artifacts on CT images: relationship between streak artifacts and mA s values. *Med Phys*. 2009;36:492-499.
11. Imai K, Ikeda M, Enchi Y, Niimi T. Quantitative assessment of image noise and streak artifact on CT image: comparison of z-axis automatic tube current modulation technique with fixed tube current technique. *Comput Med Imaging Graph*. 2009;33:353-358.
12. Kitaguchi S, Imai K, Ueda S, et al. Quantitative evaluation of metal artifacts on CT images on the basis of statistics of extremes. *Japanese J Radiol Technol*. 2016;72:402-409.
13. Kasai R, Yamada K. Application of Hamiltonian Monte Carlo method to metal artifact quantitative evaluation in computed tomography (CT). *Japanese J Radiol Technol*. 2017;73:654-663.
14. Takada K, Ichikawa K, Banno S, Otobe K. Suggestion of the relative artifact index for noise-independent evaluation of the streak artifact. *Japanese J Radiol Technol*. 2018;74:315-325.
15. Imai K, Ikeda M, Enchi Y, Niimi T. A detection method for streak artifacts and radiological noise in a non-uniform region in a CT image. *Phys Medica*. 2010;26:157-165.
16. Nomura Y, Watanabe H, Kamiyama Y, Kurabayashi T. Physical quality evaluation of voxel values in cone-beam computed tomography for dental use: three-dimensional fluctuation of voxel values in uniform materials placed inside a phantom. *Oral Radiol*. 2014;30:226-235.

17. Yampri P, Sotthivirat S, Gansawat D, et al. Performance comparison of bone segmentation on dental CT images. In: Lim CT, Goh JCH, eds. *Proceedings of the 13th International Conference on Biomedical Engineering*, Berlin, Heidelberg: Springer Berlin Heidelberg; 2009:665-668.
18. Matsuyama J, Tanaka R, Iizawa F, et al. Clinical and radiographic findings and usefulness of computed tomographic assessment in two children with regional odontodysplasia. *Case Rep Dent*. 2014;2014:1-5.
19. Mann HB, Whitney DR. On a test of whether one of two random variables is stochastically larger than the other. *Ann Math Stat*. 1947;18:50-60.
20. Guilford JP. *Fundamental Statistics in Psychology and Education*. New York: McGraw-Hill; 1942.
21. White SC, Pharoah MJ. *Oral Radiology: Principles and Interpretation*. St. Louis, MO: Mosby/Elsevier; 2009.
22. Katsumata A, Hirukawa A, Noujeim M, et al. Image artifact in dental cone-beam CT. *Oral Surg Oral Med Oral Pathol Oral Radiol Endod*. 2006;101:652-657.
23. Bayrak S, Orhan K, Kursun Çakmak ES, et al. Evaluation of a metal artifact reduction algorithm and an optimization filter in the estimation of peri-implant dehiscence defects by using cone beam computed tomography: an in-vitro study. *Oral Surg Oral Med Oral Pathol Oral Radiol*. 2020;130:209-216.
24. Araki K, Okano T. The effect of surrounding conditions on pixel value of cone beam computed tomography. *Clin Oral Implants Res*. 2013;24:862-865.
25. Kawamata R, Sakurai T, Kashima I. Basic study of three-dimensional fine vascular structural analysis based on morphological processing. *Oral Radiol*. 2013;29:40-49.

Reprint requests:

Yoshikazu Nomura
Oral and Maxillofacial Radiology
Graduate School
Tokyo Medical and Dental University
1-5-45 Yushima
Bunkyo-ku
Tokyo 113-8549
Japan.
ynmr.orad@tmd.ac.jp